ISSN 1063-7737, Astronomy Letters, 2016, Vol. 42, No. 11, pp. 752–755. © Pleiades Publishing, Inc., 2016.
Original Russian Text © A.V. Dodin, 2016, published in Pis'ma v Astronomicheskii Zhurnal, 2016, Vol. 42, No. 11, pp. 826–830.

Oblique MHD Shock near the Surface of Young Stars

A. V. Dodin*

Sternberg Astronomical Institute, Moscow State University, Universitetskii pr. 13, Moscow, 119992 Russia

Received May 16, 2016

Abstract—The dependence of the spectrum of a hot spot at the surface of accreting young stars on the angle at which the material falls onto the star is considered. For typical parameters of T Tauri stars the structure of the shock at oblique incidence has been found to be no different from its structure at normal incidence, but at the same time the inclination, along with the gas density and velocity, is shown to be an independent accretion parameter the changes in which lead to noticeable changes in the hot-spot spectrum.

DOI: 10.1134/S1063773716110013

Keywords: *shocks, stellar atmospheres, accretion, T Tauri stars.*

INTRODUCTION

The currently existing calculations of the structure and spectrum of accretion regions in T Tauri stars were performed under the assumption of normal incidence of the material on their surface (Calvet and Gullbring 1998; Dodin 2015). In this case, the magnetic field whose field lines are perpendicular to the surface channels the gas flow but does not affect the structure of the emerging shock. However, the material falls onto the star at a certain angle to its surface even in the simplest case of a dipole field. The work is aimed at revealing the changes in the hot-spot spectrum to which oblique incidence of the material on the stellar surface leads. Recall that the stellar atmosphere located under the shock and heated by stellar radiation is meant by the hot spot.

Let us first specify the domain of physical parameters typical of magnetospheric accretion onto magnetized young stars. The typical magnetic field strength in the accretion region is 1–8 kG (Chuntonov et al. 2007; Donati et al. 2008; Dodin et al. 2012). The typical preshock gas velocity V_0 lies within the range 200–400 km s^{-1}. The total preshock number density of atomic nuclei is $N_0 \sim 10^{11}$–10^{13} cm^{-3} (Kastner et al. 2002; Schmitt et al. 2005; Dodin et al. 2013), corresponding to a gas density $\rho_0 \sim 10^{-13}$–10^{-11} g cm^{-3}. Consequently, the ratio of the kinetic energy density to the magnetic energy density $\delta = \frac{\rho_0 V_0^2}{2} / \frac{B^2}{8\pi} \lesssim 0.1$. At such parameters the gas motion in a magnetic field at an angle to the stellar surface gives rise to the so-called slow MHD shock.

General questions about the structure of MHD shocks were discussed in the book of Somov (2006) and in the papers of Ledentsov and Somov (2012, 2015), while we are primarily interested in the radiation emerging behind the shock front. This radiation has already been calculated by Lamzin (1998), but only for normal incidence. In the next section we will show that Lamzin's results can be applied to the case of oblique incidence at $\delta \lesssim 0.1$.

THE STRUCTURE OF AN OBLIQUE MHD SHOCK

Figure 1 presents a scheme of the plasma flow through an oblique shock. Let us assign the sub-

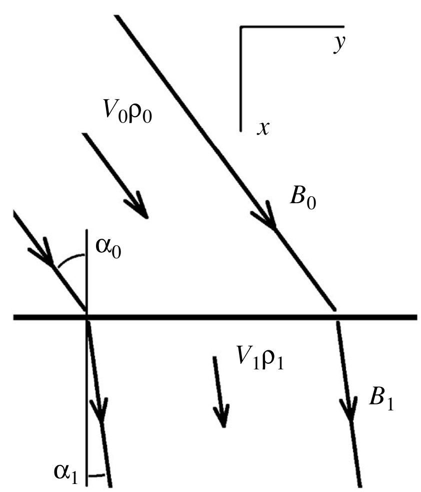

Fig. 1. Scheme of the flow through an oblique MHD shock. The shock front is indicated by the thick horizontal line.

*E-mail: dodin_nv@mail.ru

scripts 0 and 1 to the preshock and postshock physical parameters, respectively. To be specific, let us introduce a Cartesian coordinate system whose x axis is perpendicular to the discontinuity plane and is directed toward the star and whose y axis lies in the discontinuity plane in such a way that the velocity component $V_{z0} = 0$. Using the standard notation for physical quantities, let us write the conditions at the MHD discontinuity (see, e.g., Somov 2006):

$$\{B_x\} = 0, \tag{1}$$

$$\{\rho V_x\} = 0, \tag{2}$$

$$\{V_x B_y - V_y B_x\} = 0, \tag{3}$$

$$\left\{\rho V_x V_y - \frac{B_x B_y}{4\pi}\right\} = 0, \tag{4}$$

$$\left\{P + \rho V_x^2 + \frac{B^2}{8\pi}\right\} = 0, \tag{5}$$

$$\left\{\rho V_x \left(\frac{V^2}{2} + \varepsilon + \frac{P}{\rho}\right) + \frac{1}{4\pi}\left(B^2 V_x - (\mathbf{v}\cdot\mathbf{B})B_x\right)\right\} = 0. \tag{6}$$

Recall that $\{X\}$ denotes the difference between the values of quantity X behind and ahead of the discontinuity.

From conditions (1)–(4) for the plasma flowing into the discontinuity along the magnetic field we can calculate the relation between the physical quantities ahead of and behind the discontinuity:

$$B_{x1} = B_{x0},$$

$$B_{y1} = B_{x0}\tan\alpha_1,$$

$$\tan\alpha_1 = \frac{1-\delta}{1-k\delta}\tan\alpha_0,$$

$$V_{x1} = kV_{x0},$$

$$V_{y1} = kV_{x0}\tan\alpha_1.$$

Here, α is the inclination of the streamlines to the normal. The quantity $k = \rho_0/\rho_1$ is determined from conditions (5) and (6), which in the case of a strong shock ($P_0 \ll \rho_0 V_0^2$) in a monoatomic ideal gas ($\varepsilon = 1.5P/\rho$) lead to the equation

$$5\delta(1-k)k + \frac{5}{2}k\tan^2\alpha_0\left[1 - \left(\frac{1-\delta}{1-k\delta}\right)^2\right] + k^2\delta\left[1 + \tan^2\alpha_0\left(\frac{1-\delta}{1-k\delta}\right)^2\right] = \delta\left(1+\tan^2\alpha_0\right).$$

In our case, a fortiori $k\delta < 1$; the equation is then reduced to a quartic equation and must have four roots. The trivial root $k = 1$ corresponds to the absence of a discontinuity. Two more roots have no physical meaning, because they correspond to a rarefaction wave. The fourth root corresponds to a compression wave and when expanded to the first power in δ is

$$k \approx \frac{1}{4}\left(1 + \frac{9}{32}\delta\sin^2\alpha_0\right). \tag{7}$$

The structure of the cooling postshock gas will be determined by the parameters immediately behind the shock front: the density ρ_1 and temperature. The latter can be expressed as

$$T_1 \approx T_{n1}\left(1 + \frac{1}{16}\delta\sin^2\alpha_0\right), \tag{8}$$

where T_{n1} is the postshock temperature in the case of normal incidence of the material. To calculate the structure of the hot spot, we will also need to know the pressure on its outer boundary:

$$P_{\rm hs} = P_1 + \rho_1 V_1^2 \approx P_0 + \rho_0 V_0^2\left(1 - \frac{15}{32}\delta\sin^2\alpha_0\right). \tag{9}$$

It can be seen from the derived expressions (7) and (8) that at $\delta < 0.1$ the changes in shock structure will be less than 3%. This means that the distribution of parameters for the cooling postshock gas along the magnetic field lines is virtually independent of the angle of incidence of the material. The structure of the postshock region is determined only by the initial conditions (7) and (8) and gas cooling processes. Such a structure was calculated by Lamzin (1998), who assumed the gas to be optically thin at all frequencies. Consequently, under the same assumptions the structure of the postshock region *along the streamlines* will correspond to the structure calculated for normal incidence. Such a simple result is attributable to the presence of a strong magnetic field that channels the material. For comparison, note that the postshock temperature in the case of an oblique hydrodynamic shock (without a magnetic field) would be determined by the normal velocity component: $T_1 \propto V_{x0}^2 \propto \cos^2\alpha_0$, i.e., T_1 would exhibit a strong dependence on the angle (Landau and Lifshitz 1986).

The spectrum of the region behind the MHD shock front is determined by its structure and will not change compared to normal incidence. However, the postshock region will be thinner along the normal, which will lead to a decrease in the intensity that will be

$$I(\mu) = I_n(\mu)\cos\alpha_0, \tag{10}$$

where $I_n(\mu)$ is the angular distribution of the radiation intensity in the case of normal incidence of the

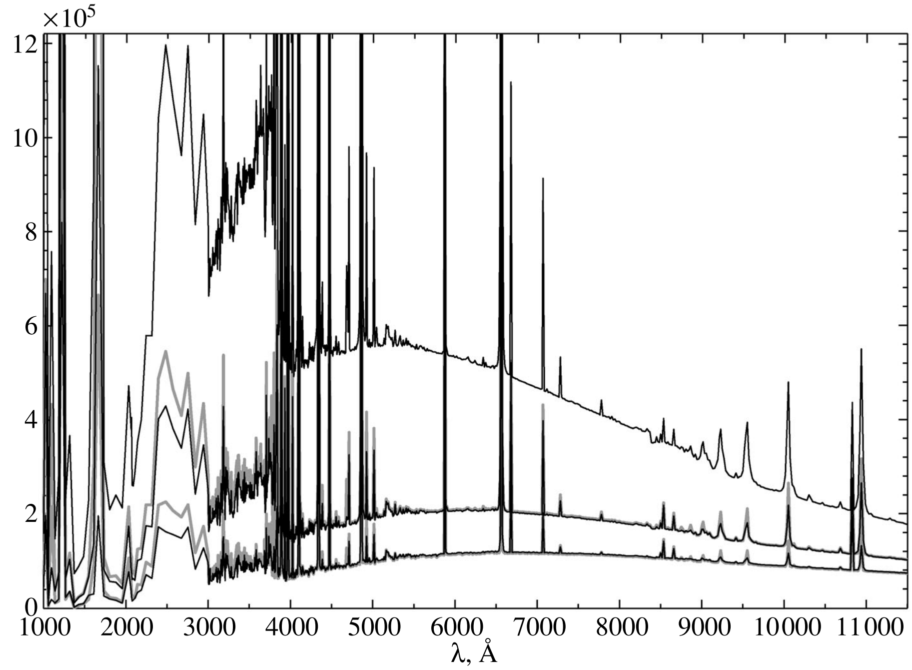

Fig. 2. Spectral energy distribution of the hot spot for the models $\Pi_{\rm acc} = \{300,\ 12.5,\ 1\}$ (upper black line), $\Pi_{\rm acc} = \{300,\ 12.5,\ 0.3\}$ (middle black line), $\Pi'_{\rm acc} = \{300,\ 12,\ 1\}$ (middle gray line), $\Pi_{\rm acc} = \{300,\ 12.5,\ 0.1\}$ (lower black line), and $\Pi'_{\rm acc} = \{300,\ 11.5,\ 1\}$ (lower gray line). $\Pi_* = \{4000,\ 4.0,\ 1.25,\ 2.0\}$. The Eddington H_λ flux in erg s^{-1} cm^{-2} Å^{-1} sr^{-1} is along the vertical axis.

gas. The external pressure on the hot-spot boundary will be

$$P_{\rm hs} \approx \rho_0 V_0^2, \tag{11}$$

because the remaining terms in (9) may be neglected. Consequently, in the case of a strong magnetic field, the inclination of the magnetic field lines to the discontinuity surface leads to a decrease in the intensity of the radiation incident on the hot spot without any change in the pressure applied to its outer boundary.

THE HOT-SPOT SPECTRUM IN THE CASE OF AN OBLIQUE SHOCK

Using the boundary conditions (10) and (11) and the methods described in Dodin (2015), we calculated the hot-spot structure and spectrum for the accretion parameters $V_0 = 300$ km s^{-1} and $\log N_0 = 12.5$ and a set of $\cos\alpha_0 = 0.1{-}1.0$. The stellar parameters are $T_{\rm eff} = 4000$ K and $\log g = 4.0$, the mixing-length parameter is $\alpha_{MLT} = 1.25$, the microturbulence is $V_t = 2$ km s^{-1}, and the elemental abundances are solar. Below, for brevity, we will denote the accretion parameters as $\Pi_{\rm acc} = \{V_0({\rm km\ s^{-1}}),\ \log N_0,\ \cos\alpha_0\}$, and the stellar parameters as $\Pi_* = \{T_{\rm eff}({\rm K}),\ \log g,\ \alpha_{MLT},\ V_t({\rm km\ s^{-1}})\}$. The results of our calculations for the continuum and some of the most important spectral lines are represented by the solid curves in Figs. 2 and 3. It it can be seen from these figures that the hot-spot radiation is attenuated with increasing angle α_0, which is explained by the decrease in $I(\mu)$.

It should be noted that the shape of the shock spectrum $I_n(\mu)$ is almost independent of the infalling gas density and, to a first approximation, $I_n(\mu) \propto \rho_0 \propto N_0$ (Lamzin 1998). Thus, $I(\mu)$ equally depends on N_0 and $\cos\alpha_0$. It could then be assumed that the set $\Pi'_{\rm acc} = \{V_0,\ \log(N_0\cos\alpha_0),\ 1\}$ should be used instead of $\Pi_{\rm acc} = \{V_0, \log N_0, \cos\alpha_0\}$, because both sets $\Pi_{\rm acc}$ and $\Pi'_{\rm acc}$ give identical spectra $I(\mu)$. For example, the models $\Pi_{\rm acc} = \{300,\ 12.5,\ 0.3\}$ and $\Pi_{\rm acc} = \{300,\ 12.5,\ 0.1\}$ have virtually the same spectrum of the incoming radiation as do the models $\Pi'_{\rm acc} = \{300,\ 12.0,\ 1\}$ and $\Pi'_{\rm acc} = \{300,\ 11.5,\ 1\}$, respectively. As can be seen from Fig. 2, the continuum emissions for the models $\Pi_{\rm acc}$ and $\Pi'_{\rm acc}$ in the visible spectral range closely coincide with one another. However, differences appear in spectral lines and in the ultraviolet (see Figs. 2 and 3). This is because the upper boundary condition, apart from the radiation $I \propto \rho_0\cos\alpha_0$, includes the pressure $P_{\rm hs} \propto \rho_0$ that does not depend on $\cos\alpha_0$. An elevated pressure in the model $\Pi_{\rm acc}$ in comparison with $\Pi'_{\rm acc}$ leads to a weakening of the He II lines (in qualitative agreement with Saha's formula) and to a greater line broadening (see Fig. 3). Consequently, the radiation

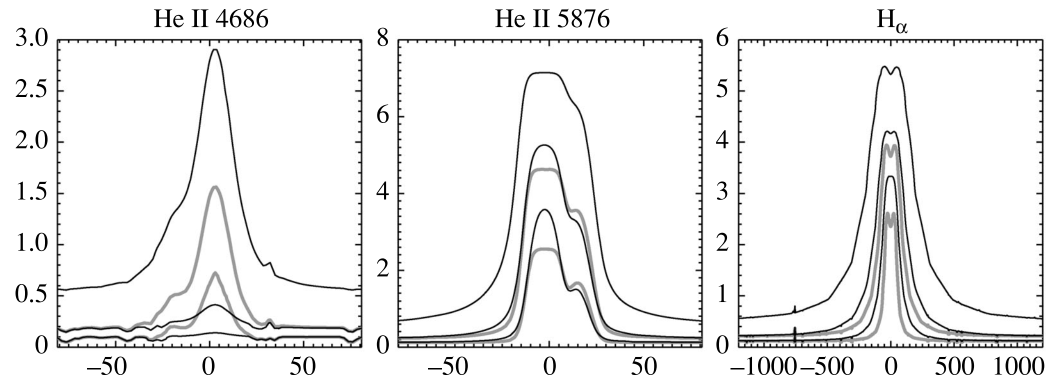

Fig. 3. Profiles of some of the most interesting lines. The model parameters are the same as those in Fig. 2. The Eddington H_λ flux in erg s^{-1} cm^{-2} $Å^{-1}$ sr^{-1} is along the vertical axis. The radial velocity in km s^{-1} is along the horizontal axis.

originating in the upper layers of the hot spot, where the external pressure $P_{\rm hs}$ dominates, can be described only by the set $\Pi_{\rm acc}$, and, as was shown previously (Dodin 2015), this radiation is almost independent of the stellar parameters Π_*. The intrinsic hydrostatic pressure of the stellar atmosphere increases in importance as we go into the deeper layers. Therefore, the deeper the radiation originates, the smaller the differences between the spectra calculated with the sets of parameters $\Pi_{\rm acc}$ and $\Pi'_{\rm acc}$, and the bigger the role of Π_*.

CONCLUSIONS

We showed that oblique incidence of material on the surface of a star leads to a decrease in the effective temperature of the hot spot, mimicking a decrease in the infalling gas density in the model with normal incidence as $\rho_0 \cos\alpha_0$. However, for the spectral lines that are formed in the upper layers of the hot spot, for example, for the emission in He II lines, such a combination of parameters is impossible—the angle must be considered as yet another accretion parameter.

ACKNOWLEDGMENTS

This study was financially supported by the Russian Foundation for Basic Research (project no. 16-32-00794 mol_a). The work was financed in part by the Program for Support of Leading Scientific Schools (NSh-261.2014.2).

REFERENCES

1. N. Calvet and E. Gullbring, Astrophys. J. **509**, 802 (1998).
2. G. A. Chuntonov, D. A. Smirnov, and S. A. Lamzin, Astron. Lett. **33**, 38 (2007).
3. A. V. Dodin, Astron. Lett. **41**, 196 (2015).
4. A. V. Dodin, S. A. Lamzin, and G. A. Chuntonov, Astron. Lett. **38**, 167 (2012).
5. A. V. Dodin, S. A. Lamzin, and T. M. Sitnova, Astron. Lett. **39**, 315 (2013).
6. J.-F. Donati, M. M. Jardine, S. G. Gregory, P. Petit, F. Paletou, J. Bouvier, C. Dougados, F. Ménard, et al., Mon. Not. R. Astron. Soc. **386**, 1234 (2008).
7. J. H. Kastner, D. P. Huenemoerder, N. S. Schulz, and C. R. Canizares, Astrophys. J. **567**, 434 (2002).
8. S. A. Lamzin, Astron. Rep. **42**, 322 (1998).
9. L. D. Landau and E. M. Lifshitz, *Course of Theoretical Physics,* Vol. 6: *Fluid Mechanics* (Nauka, Moscow, 1986; Pergamon, Oxford, 1987), p. 345.
10. L. S. Ledentsov and B. V. Somov, Astron. Lett. **38**, 744 (2012).
11. L. S. Ledentsov and B. V. Somov, Adv. Space Res. **56**, 2779 (2015).
12. J. H. M. M. Schmitt, J. Robrade, J.-U. Ness, F. Favata, and B. Stelzer, Astron. Astrophys. **432**, L35 (2005).
13. B. V. Somov, *Plasma Astrophysics* (Springer, Berlin, 2006), Vol. 1, p. 277.

Translated by V. Astakhov